Science Advances
AAAS

Supplementary Materials for

Amyloid fibril structures and ferroptosis activation induced by ALS-causing SOD1 mutations

Li-Qiang Wang *et al.*

Corresponding author: Cong Liu, liulab@sioc.ac.cn; Yi Liang, liangyi@whu.edu.cn

Sci. Adv. **10**, eado8499 (2024)
DOI: 10.1126/sciadv.ado8499

The PDF file includes:

Other Supplementary Material for this manuscript includes the following:

Supplementary Materials

table S1.

The primers designed for full-length human SOD1 with H46R mutation or G85R mutation.

S-H46R	5’ CATGGATTCCGTGTTCATGAGTTTGG3’
A-H46R	5’ CTCATGAACACGGAATCCATGCAGG3’
S-G85R	5’ CATGGATTCCGTGTTCATGAGTTTGG3’
A-G85R	5’ GGAGACTTGCGCAATGTGACTGCTG’

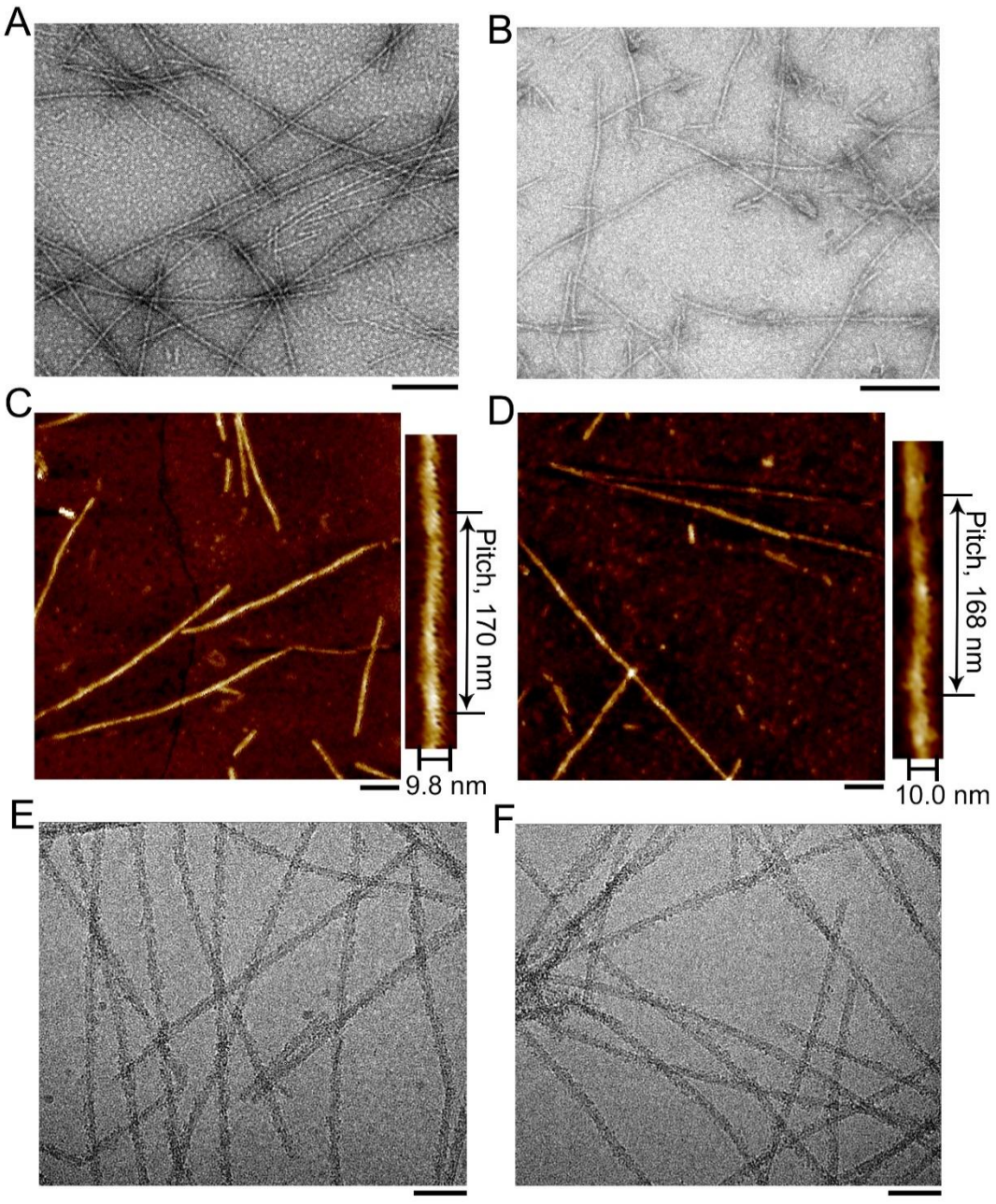

figure S1.

Comparison of the images of H46R fibrils and G85R fibrils. (**A** and **B**) Negative-staining TEM images of amyloid fibrils produced from ALS-causing SOD1 mutant proteins H46R (A) and G85R (B). (**C** and **D**) AFM images of amyloid fibrils assembled from H46R (C) and G85R (D). Enlarged sections of (C) and (D) (right) showing the H46R fibril (C) and the G85R fibril (D) intertwined into a left-handed helix, with a fibril full width of 9.8 ± 1.0 nm and 10.0 ± 1.4 nm, respectively, and a helical pitch of 170 ± 9 nm and 168 ± 7 nm, respectively. The helical pitch and fibril width were

measured and expressed as the mean ± SD of values obtained in n = 8 biologically independent measurements. (**E** and **F**) Raw cryo-EM images of amyloid fibrils assembled from H46R (E) and G85R (F). The scale bars represent 200 nm (A and B) and 100 nm (C to F), respectively.

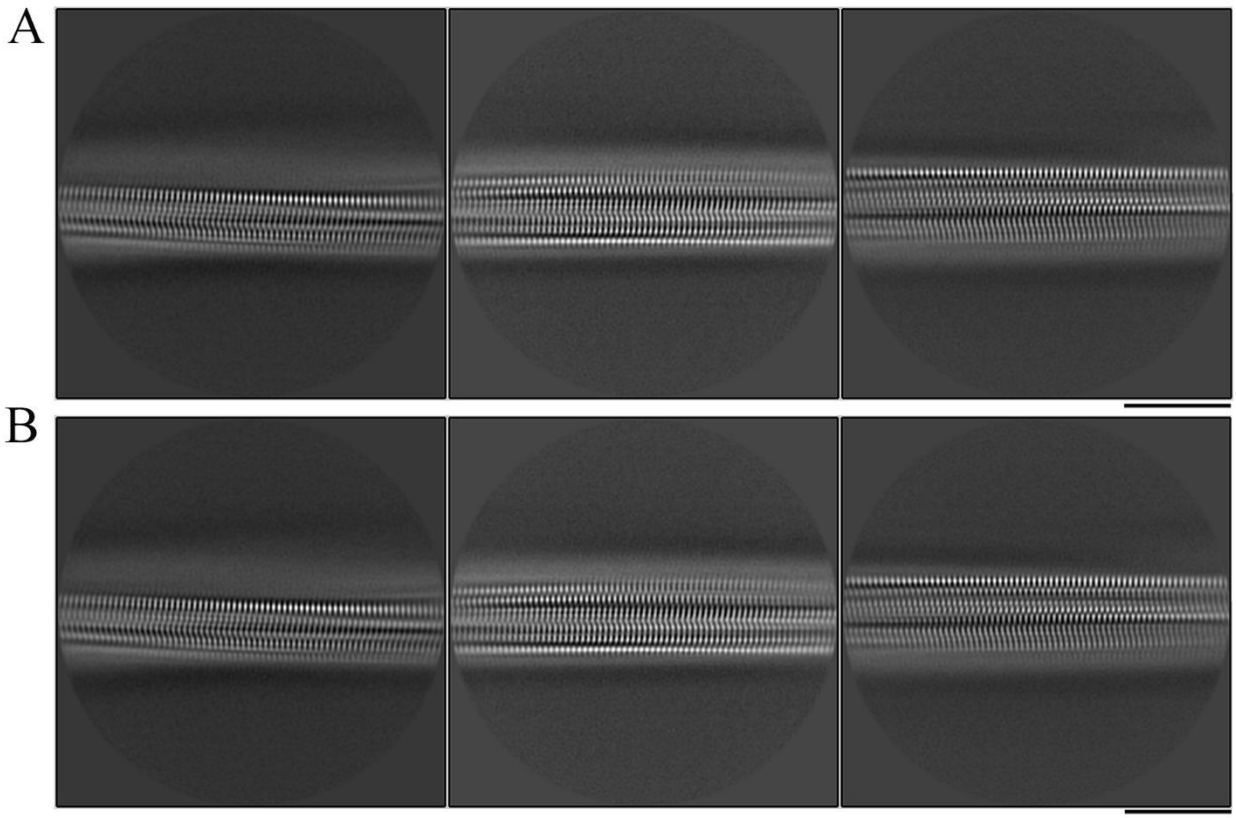

figure S2.

Comparison of the cryo-EM images of the H46R fibril and the G85R fibril. (**A** and **B**) Reference-free 2D class averages of the H46R fibril (A) and the G85R fibril (B) both showing a single protofilament intertwined. Scale bar, 10 nm.

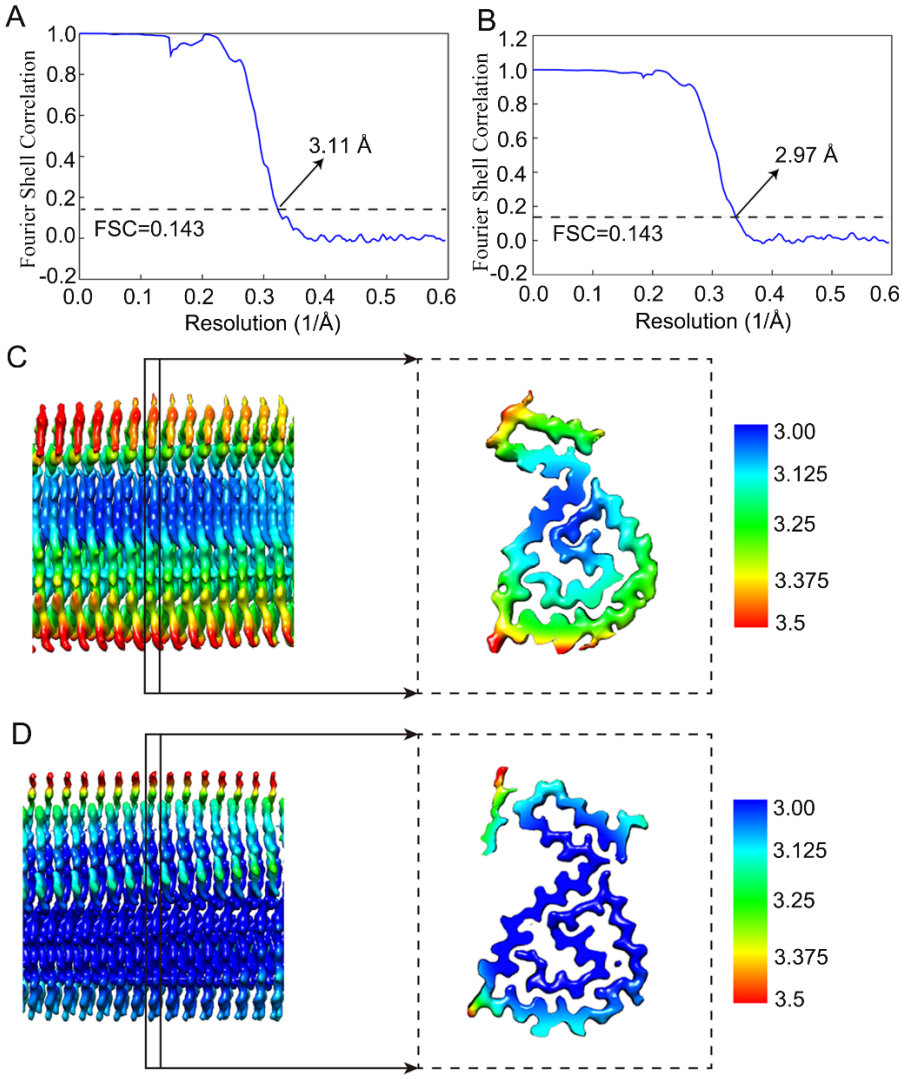

figure S3.

Global (A and B) and local resolution (C and D) estimates for the reconstructions of the H46R fibril and the G85R fibril. (**A** and **B**) The reconstruction was reworked and gold-standard refinement was used for estimation of the density map resolution. The global resolutions of 3.11 Å for the H46R fibril (A) and 2.97 Å for the G85R fibril (B) were calculated using two Fourier shell correlation (FSC) curves (blue) cut-off at 0.143. (**C** and **D**) The density maps of H46R fibrils (C) and G85R fibrils (D) are colored according to local resolution estimated by ResMap. The enlarged cross sections show the left top view of the density maps of a single protofilament in the H46R fibril (C) and a single protofilament in the G85R fibril (D). The color keys on the right show the local structural resolution in angstroms (Å) and the colored maps indicate the local resolution ranging from 3.0 to 3.5 Å.

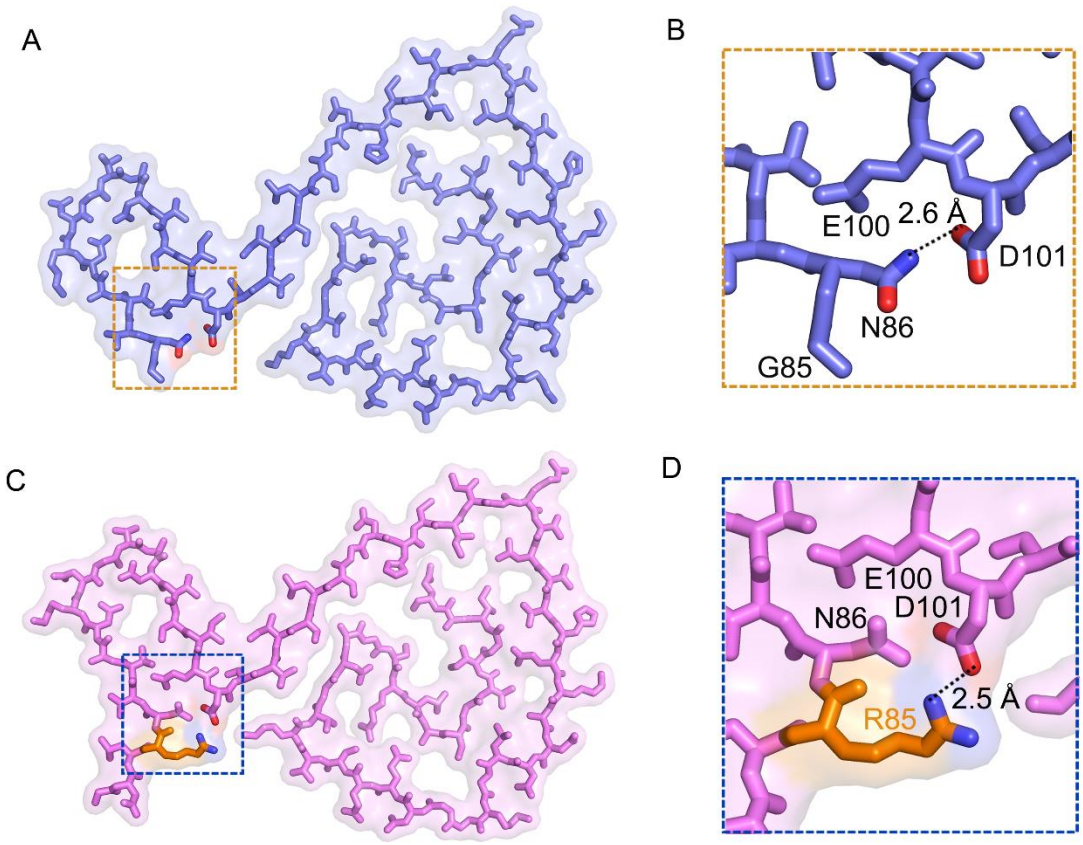

figure S4.

Close-up view of the stick representations of the structures of the H46R fibril and the G85R fibril stabilized by a hydrogen bond (A and B) and an intramolecular salt bridge (C and D), respectively. (**A**) A space-filled model overlaid onto a stick representation of the H46R fibril in which a single protofilament is shown in blue. Asp/Asn pairs that form a hydrogen bond are highlighted in red (oxygen atom in Asp) and blue (nitrogen atom in Asn), and the hydrogen bond region is magnified in (B). (**B**) A magnified top view of the hydrogen bond region of an H46R protofilament, where a hydrogen bond is formed between Asp101 and Asn86, with a distance of 2.6 Å. (**C**) A space-filled model overlaid onto a stick representation of the G85R fibril in which a single protofilament is shown in magenta. Asp/Arg pairs that form a new salt bridge are highlighted in red (oxygen atom in Asp) and blue (nitrogen atom in Arg), and the salt bridge region is magnified in (D). (**D**) A magnified top view of the salt bridge region of an G85R protofilament, where a strong salt bridge is formed between Asp101 and Arg85, with a distance of 2.5 Å. Arg85 in G85R variant is highlighted in orange.

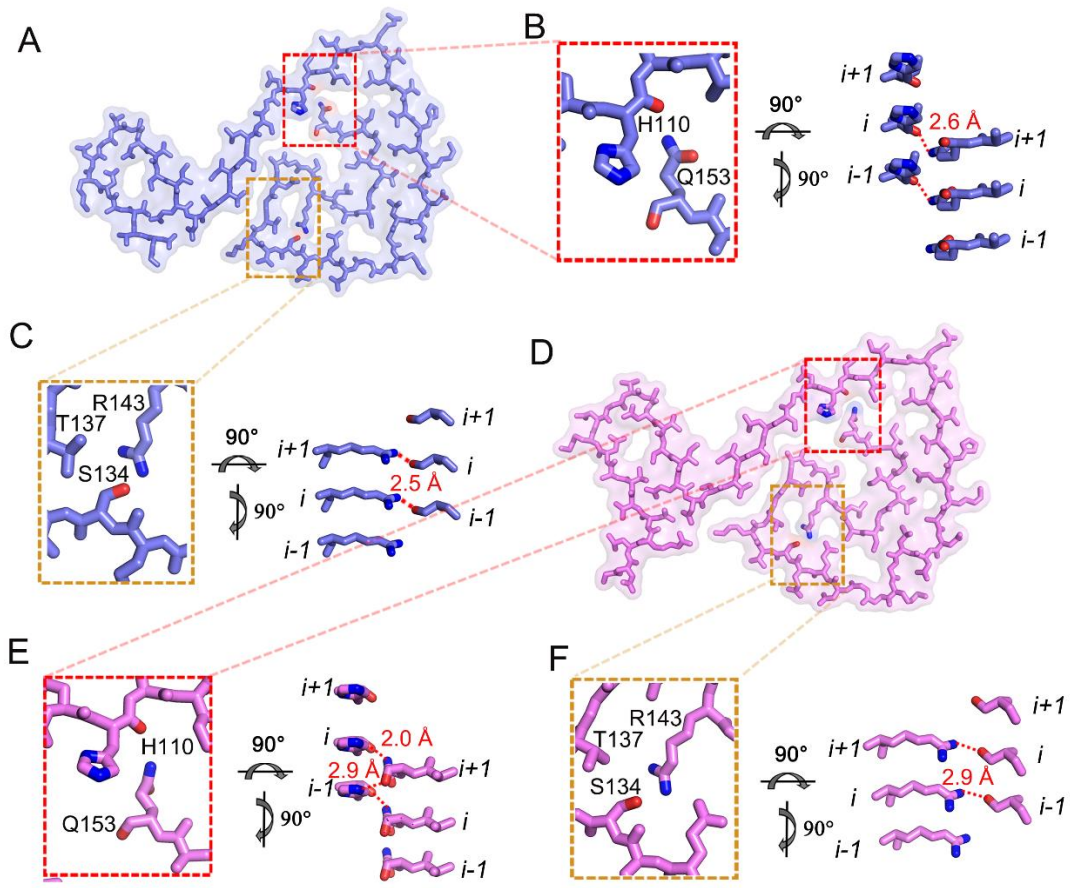

figure S5.

Close-up view of the stick representations of the structures of the H46R fibril and the G85R fibril stabilized by two hydrogen bonds (A to C) and three hydrogen bonds (D to F), respectively. (**A**) A space-filled model overlaid onto a stick representation of the H46R fibril in which a single protofilament is shown in blue. His/Gln pairs and Ser/Arg pairs that form hydrogen bonds are highlighted in red (oxygen atoms in His and Ser) and blue (nitrogen atoms in Gln and Arg), and two hydrogen bond regions are magnified in (B and C). (**B** and **C**) Magnified top views of the two hydrogen bond regions of an H46R protofilament, where two pairs of amino acids (His110 and Gln153; and Ser134 and Arg143) form two hydrogen bonds. Two side views (right) highlighting a hydrogen bond between the main chain of His110 from the molecular layer (*i*) and Gln153 from the adjacent molecular layer (*i* + 1), with a distance of 2.6 Å (red), or between Ser134 from the molecular layer (*i*) and Arg143 from the adjacent molecular layer (*i* + 1), with a distance of 2.5 Å (red). (**D**) A space-filled model overlaid onto a stick representation of the G85R fibril in which a single

protofilament is shown in magenta. His/Gln pairs and Ser/Arg pairs that form hydrogen bonds are highlighted in red (oxygen atoms in His and Ser) and blue (nitrogen atoms in Gln and Arg), and three hydrogen bond regions are magnified in (E and F). (**E** and **F**) Magnified top views of the three hydrogen bond regions of an G85R protofilament, where two pairs of amino acids (His110 and Gln153; and Ser134 and Arg143) form three hydrogen bonds. Two side views (right) highlighting a hydrogen bond between the main chain of His110 from the molecular layer (*i*) and Gln153 from the adjacent molecular layer ($i + 1$), with a distance of 2.0 Å (red), or between His110 from the molecular layer ($i -1$) and the main chain of Gln153 from the molecular layer ($i + 1$), with a distance of 2.9 Å (red), or between Ser134 from the molecular layer (*i*) and Arg143 from the adjacent molecular layer ($i + 1$), with a distance of 2.9 Å (red).

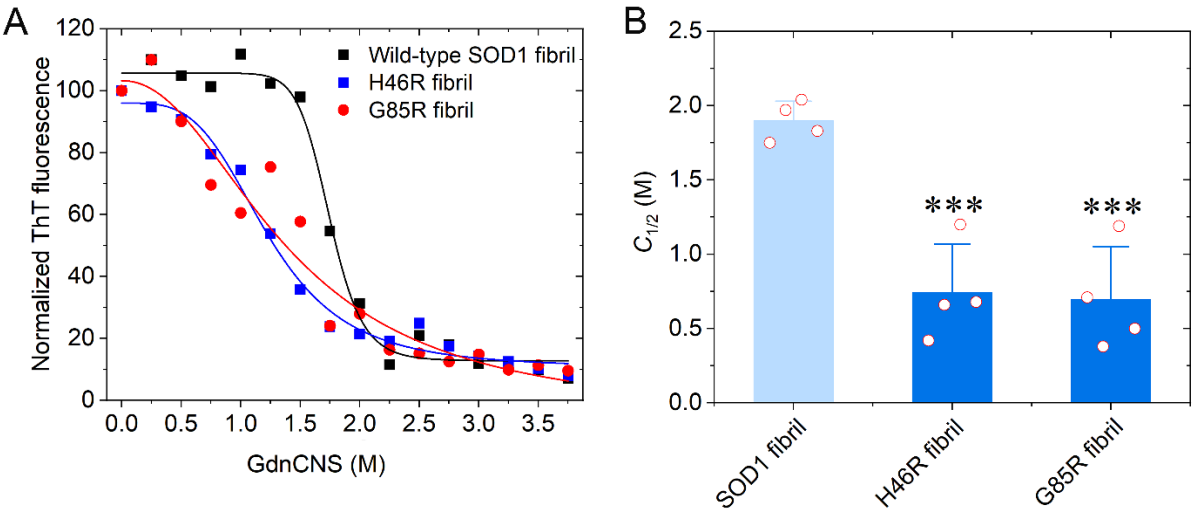

figure S6.

The H46R mutation and the G85R mutation significantly decrease the conformational stability of SOD1 fibrils. Amyloid fibrils were produced from the apo forms of recombinant wild-type SOD1 and its variants H46R and G85R incubated in 20 mM tris-HCl buffer (pH 7.4) containing 5 mM TCEP and shaking at 37 °C for 40–48 h. (**A**) GdnSCN-induced denaturation profiles were monitored for the H46R fibril (blue), the G85R fibril (red), and the wild-type SOD1 fibril (black). Samples (10 μM) of the SOD1 fibrils were incubated for 1 h at 25°C in the presence of different concentrations of GdnSCN. The concentration of GdnSCN was then adjusted to 0.35 M, followed by a ThT binding assay. The solid lines show the best sigmoidal fit for the ThT intensity-time curves. These experiments were repeated four times with different batches of fibrils and similar results. (**B**) The $C_{1/2}$ (the half-concentration at which the ThT fluorescence intensity of SOD1 fibrils is decreased by 50%) values of the H46R fibril (blue), the G85R fibril (blue), and the wild-type SOD1 fibril (light blue) (open red circles shown in scatter plots) were determined using a sigmoidal equation (*68*, *72*) using the ThT fluorescence data obtained, and are expressed as the mean ± SD of the values obtained in 4 independent experiments. The H46R fibril, $P = 0.00014$; and the G85R fibril, $P = 0.00073$. Statistical analyses were performed using two-sided Student's t-test. Values of $P < 0.05$ indicate statistically significant differences. The following notation is used throughout: $*P < 0.05$; $**P < 0.01$; and $***P < 0.001$ relative to the wild-type SOD1 fibril (a control).

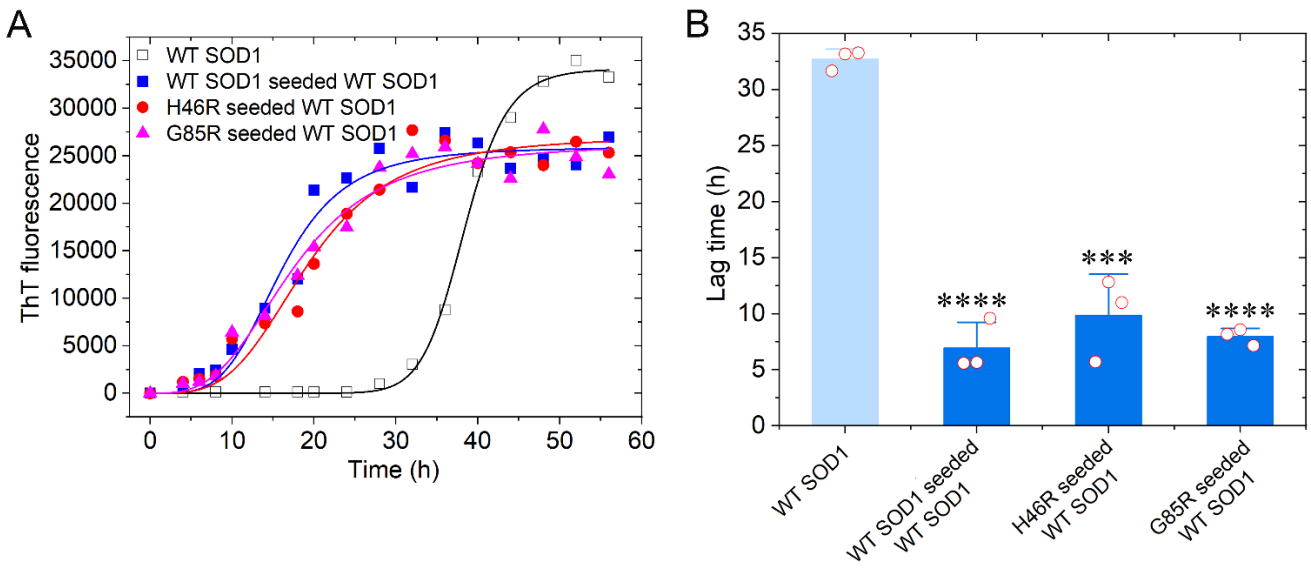

figure S7.

Wild-type SOD1 fibril seeds, H46R fibril seeds, and G85R fibril seeds significantly nucleate aggregation of wild-type SOD1 in a similar way. (**A**) Amyloid fibrils were formed from the apo form of recombinant wild-type SOD1 (30 μM) incubated in 20 mM tris-HCl buffer (pH 7.4) containing 5 mM TCEP and shaking at 37 °C for 56 h, in the absence (black) and presence of 2% (v/v) wild-type SOD1 fibril seeds (blue), 2% (v/v) H46R fibril seeds (red), or 2% (v/v) G85R fibril seeds (magenta), and then analyzed by a ThT binding assay. The solid lines show the best sigmoidal fit for the ThT intensity-time curves. These experiments were repeated three times with different batches of fibrils and similar results. (**B**) The fibril formation lag time in wild-type SOD1 in the absence (light blue) and presence of wild-type SOD1 fibril seeds (blue), H46R fibril seeds (blue), or G85R fibril seeds (blue) (open red circles shown in scatter plots) was determined using a sigmoidal equation (*68*, *72*) using the ThT fluorescence data obtained, and are expressed as the mean ± SD of the values obtained in 3 independent experiments. Wild-type SOD1 fibril-seeded wild-type SOD1, P = 0.000055; H46R fibril-seeded wild-type SOD1, P = 0.00048; and G85R fibril-seeded wild-type SOD1, P = 0.0000032. Statistical analyses were performed using two-sided Student's t-test. Values of $P < 0.05$ indicate statistically significant differences. The following notation is used throughout: *$P < 0.05$; **$P < 0.01$; ***$P < 0.001$; and ****$P < 0.0001$ relative to the lag time of wild-type SOD1 alone (a control).

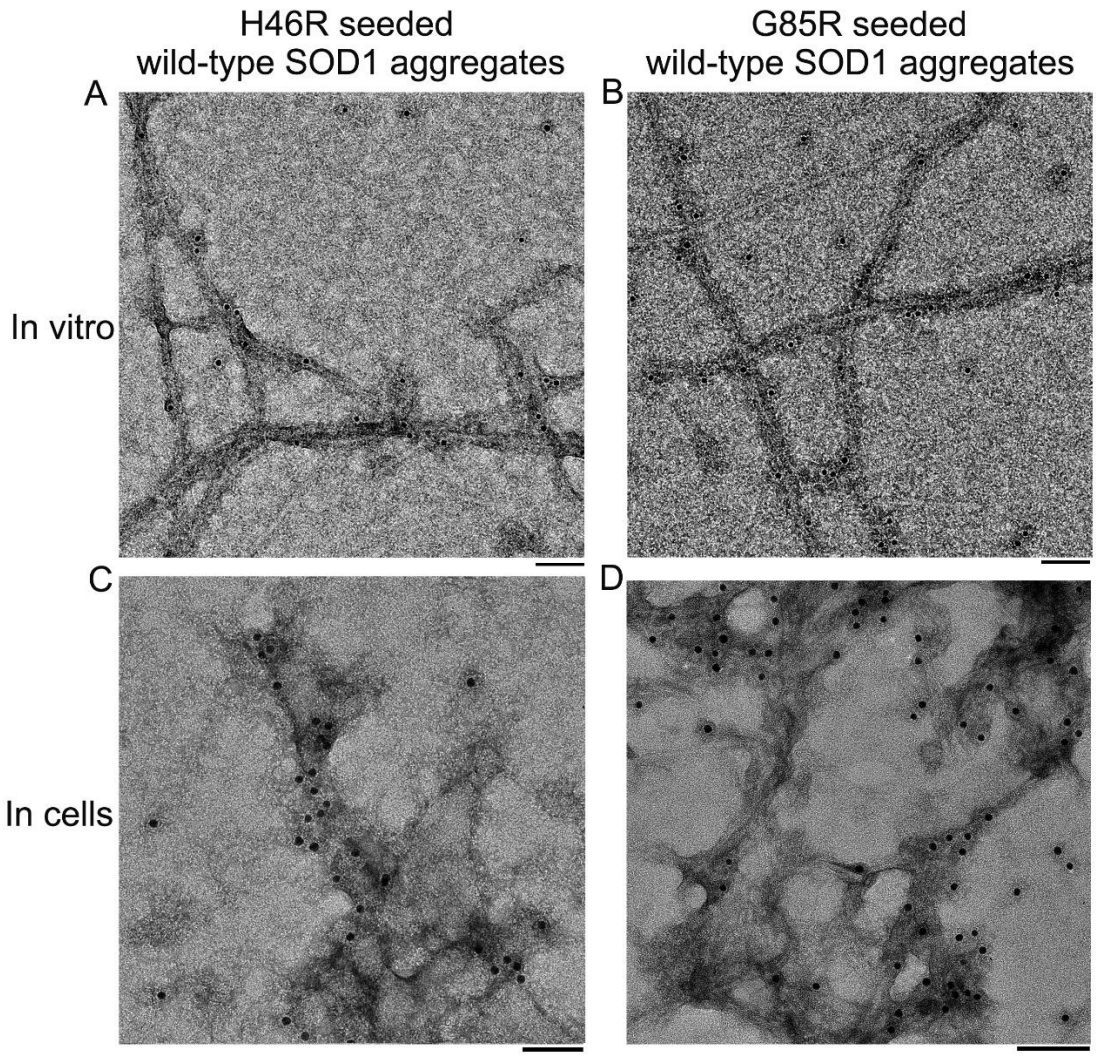

figure S8.

Anti-FLAG immunogold staining demonstrates incorporation of wild-type SOD1 into aggregates. (**A** and **B**) Immunogold electron microscopy of amyloid fibrils produced from the apo form of recombinant FLAG-tagged wild-type SOD1 (30 μM) incubated in 20 mM tris-HCl buffer (pH 7.4) containing 5 mM TCEP and shaking at 37 °C for 28 h, in the presence of 2% (v/v) H46R fibril seeds (A) and 2% (v/v) G85R fibril seeds (B), respectively, and labeled by gold particles conjugated with anti-FLAG antibody. (**C** and **D**) Immunogold electron microscopy of wild-type SOD1 aggregates purified from HEK-293T cells stably expressing FLAG-tagged wild-type SOD1 incubated with 10 μM H46R fibril seeds (C) and 10 μM G85R fibril seeds (D), respectively, for 2 days, and labeled by gold particles conjugated with anti-FLAG antibody. Scale bar, 100 nm.

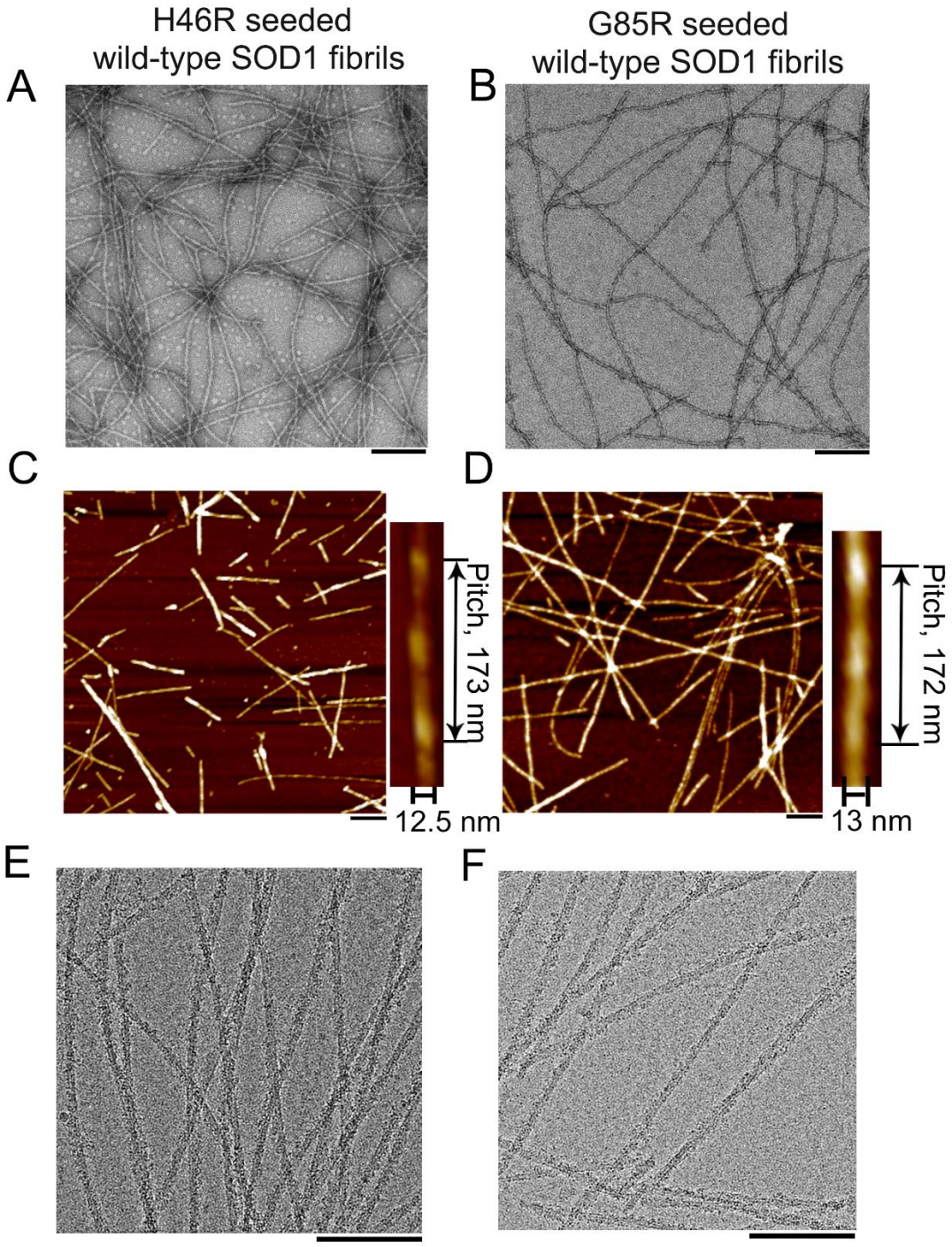

figure S9.

Wild-type SOD1 is templated into fibrils with H46R/G85R morphology. (**A** and **B**) Negative-staining TEM images of amyloid fibrils produced from the apo form of recombinant wild-type SOD1 (30 μM) incubated in 20 mM tris-HCl buffer (pH 7.4) containing 5 mM TCEP and shaking at 37 °C for 28 h, in the presence of 2% (v/v) H46R fibril seeds (A) and 2% (v/v) G85R fibril seeds (B), respectively. (**C** and **D**) AFM

images of amyloid fibrils produced from the apo form of recombinant wild-type SOD1 (30 μM) incubated in 20 mM tris-HCl buffer (pH 7.4) containing 5 mM TCEP and shaking at 37 °C for 28 h, in the presence of H46R fibril seeds (C) and G85R fibril seeds (D), respectively. Enlarged sections of (C) and (D) (right) showing the H46R fibril-seeded (C) and the G85R fibril-seeded (D) wild-type SOD1 fibrils intertwined into a left-handed helix, with a fibril full width of 13.0 ± 1.5 nm and 13.2 ± 1.0 nm, respectively, and a helical pitch of 173 ± 9 nm and 170 ± 10 nm, respectively. The helical pitch and fibril width were measured and expressed as the mean ± SD of values obtained in n = 8 biologically independent measurements. (**E** and **F**) Raw cryo-EM images of amyloid fibrils produced from the apo form of recombinant wild-type SOD1 (30 μM) incubated in 20 mM tris-HCl buffer (pH 7.4) containing 5 mM TCEP and shaking at 37 °C for 28 h, in the presence of H46R fibril seeds (E) and G85R fibril seeds (F), respectively. The scale bars represent 200 nm (A and B) and 100 nm (C to F), respectively.

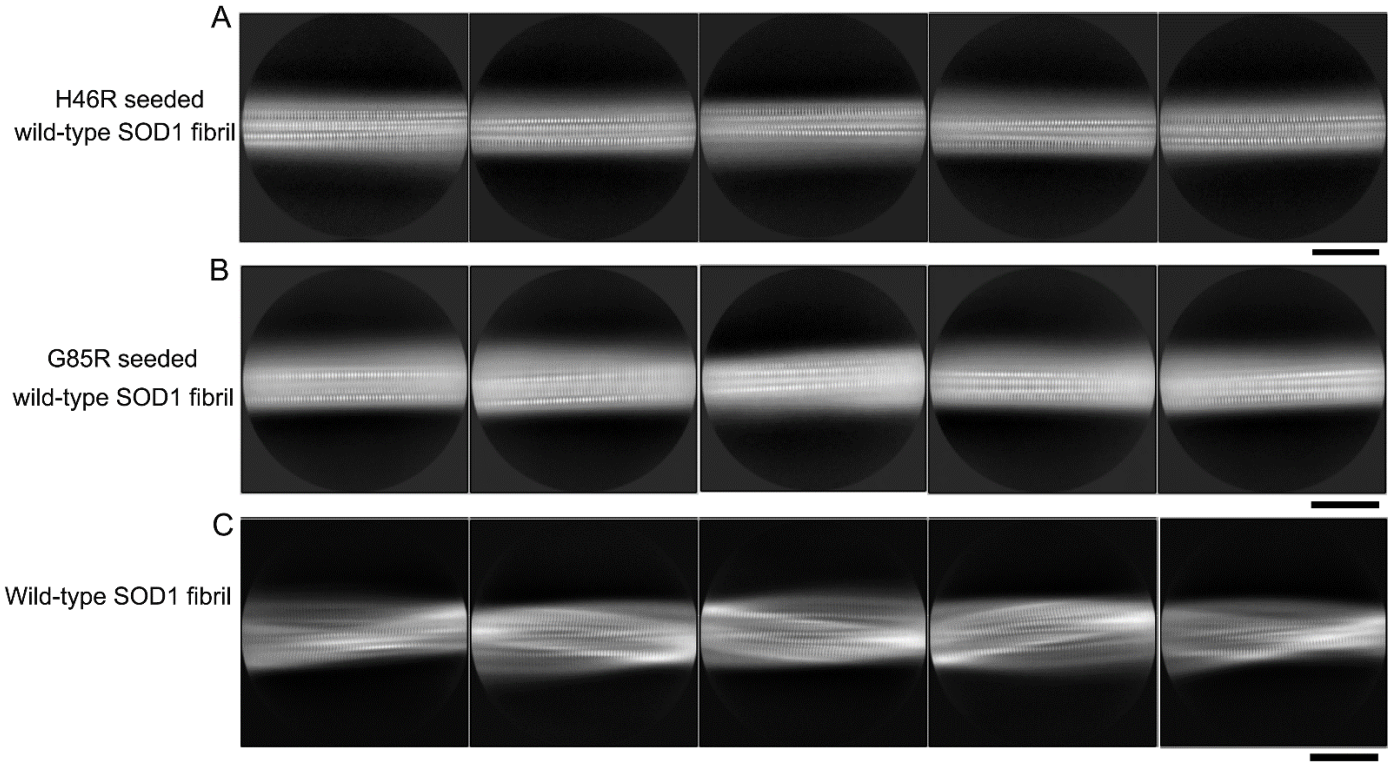

figure S10.

Wild-type SOD1 is templated into fibrils with H46R/G85R morphology rather than the wild-type SOD1 fibril morphology. (**A** and **B**) Reference-free 2D class averages of amyloid fibrils produced from the apo form of recombinant wild-type SOD1 (30 μM) incubated in 20 mM tris-HCl buffer (pH 7.4) containing 5 mM TCEP and shaking at 37 °C for 28 h, in the presence of 2% (v/v) H46R fibril seeds (B) and 2% (v/v) G85R fibril seeds (C), respectively, both showing a single protofilament intertwined. (**C**) Reference-free 2D class averages of amyloid fibrils produced from the apo form of recombinant wild-type SOD1 (30 μM) incubated in 20 mM tris-HCl buffer (pH 7.4) containing 5 mM TCEP and shaking at 37 °C for 40–48 h showing a single protofilament intertwined comprising the N- and the C-terminal segments (*43*). Under such conditions, the wild-type SOD1 fibril adopts the H46R/G85R fibril morphology. Scale bar, 10 nm.

Source Data Fig. 4A-F

Cytotoxicity of fibril seeds from H46R and G85R to SH-SY5Y neuroblastoma cells (A and B), HEK-293T cells (C and D), or HEK-293T cells stably expressing FLAG-tagged wild-type SOD1 (E and F) assessed by the CCK8 assay (A, C, and E) and the MTT assay (B, D, and F), compared with that of fibril seeds from wild-type SOD1.

Source Data Fig. 5A-I

Mitochondrial impairment induced by fibril seeds from H46R and G85R in SH-SY5Y cells, compared with that by wild-type SOD1 fibril seeds.

Source Data Fig. 5IK

(I) Box plot analyzing the relative number of mitochondria (normal/total) in SH-SY5Y cells treated with fibril seeds from H46R and G85R, compared with that with wild-type SOD1 fibril seeds.

(K) The relative amount of GPX4 in the above cell lines was determined as a ratio of the density of GPX4 band over the density of β-actin band in cell lysates and expressed as the mean ± S.D. of values obtained in three independent experiments.

Source Data Fig. 6R

The relative amount of insoluble SOD1 aggregates in HEK-293T cells stably expressing FLAG-tagged wild-type SOD1.

Source Data Fig. S1CD

The helical pitch and fibril width of the H46R fibril (C) and the G85R fibril (D).

Source Data Fig. S6A

GdnSCN-induced denaturation profiles were monitored for the H46R fibril, the G85R fibril, and the wild-type SOD1 fibril.

Source Data Fig. S6B

The $C_{1/2}$ values of the H46R fibril, the G85R fibril, and the wild-type SOD1 fibril determined using a sigmoidal equation using the ThT fluorescence data obtained.

Source Data Fig. S7A

Amyloid fibrils were formed from the apo form of recombinant wild-type SOD1 (30 μM) incubated in 20 mM tris-HCl buffer (pH 7.4) containing 5 mM TCEP and shaking at 37 °C for 56 h, in the absence and presence of 2% (v/v) wild-type SOD1 fibril seeds, 2% (v/v) H46R fibril seeds, or 2% (v/v) G85R fibril seeds, and then analyzed by a ThT binding assay.

Source Data Fig. S7B

The fibril formation lag time in wild-type SOD1 in the absence and presence of wild-type SOD1 fibril seeds, H46R fibril seeds, or G85R fibril seeds determined using a sigmoidal equation using the ThT fluorescence data obtained.

Source Data Fig. S9CD

The helical pitch and fibril width of the H46R fibril-seeded (C) and the G85R fibril-seeded (D) wild-type SOD1 fibrils.

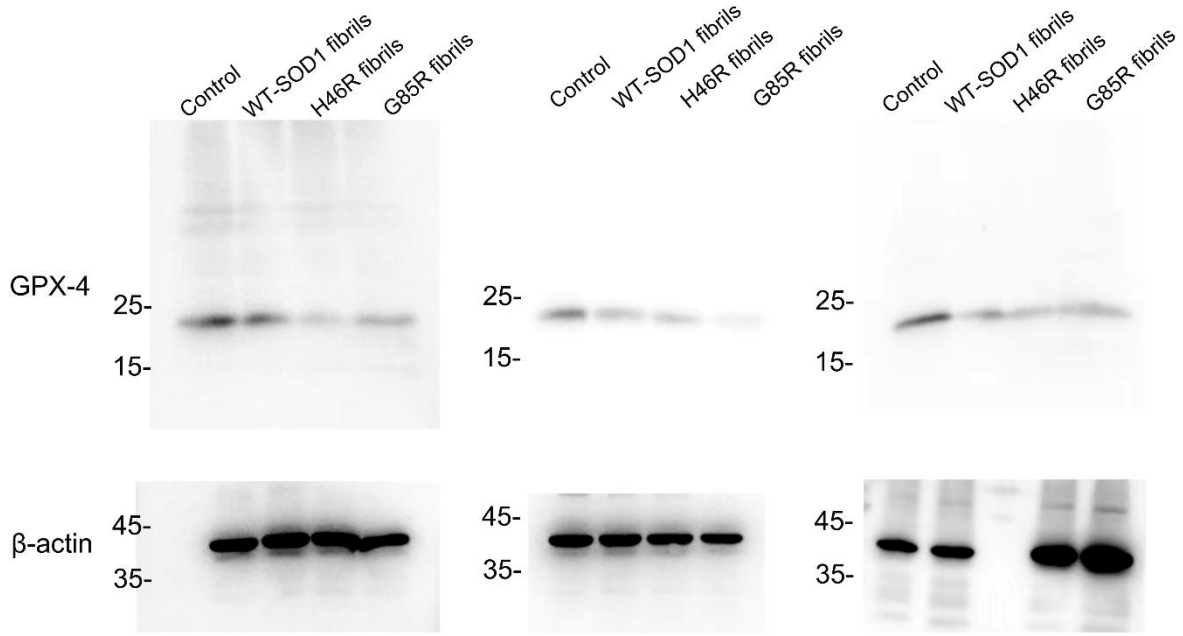

Uncropped Figure 5J

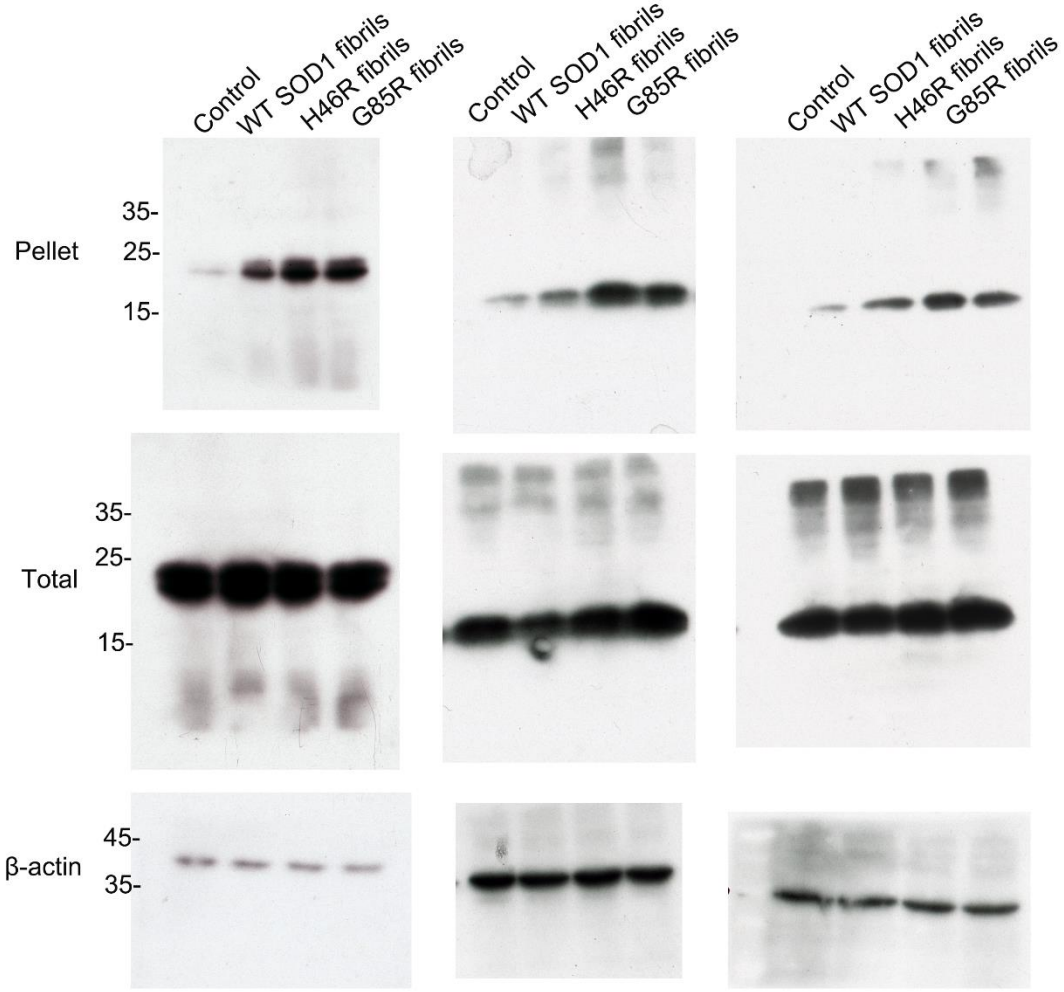

Uncropped Figure 6Q